

First-principles study of temperature-dependent diffusion coefficients: Hydrogen, deuterium, and tritium in α -Ti

Yong Lu¹ and Ping Zhang^{1,2,*}

¹*LCP, Institute of Applied Physics and Computational Mathematics,
Beijing 100088, People's Republic of China*

²*Beijing Computational Science Research Center,
Beijing 100084, People's Republic of China*

Abstract

We report the prediction of temperature-dependent diffusion coefficients of interstitial hydrogen, deuterium, and tritium atoms in α -Ti using transition state theory. The microscopic parameters in the pre-factor and activation energy of the impurity diffusion coefficients are obtained from first-principles total energy and phonon calculations including the full coupling between the vibrational modes of the diffusing atom with the host lattice. The dual occupancy case of impurity atom in the hcp matrix are considered, and four diffusion paths are combined to obtain the final diffusion coefficients. The calculated diffusion parameters show good agreement with experiments. Our numerical results indicate that the diffusions of deuterium and tritium atoms are slower than that of the hydrogen atom at temperatures above 425 K and 390 K, respectively.

PACS numbers: 63.20.dk, 63.20.D-, 66.30.-h

*Author to whom correspondence should be addressed. E-mail: zhang_ping@iapcm.ac.cn

Most metals and alloys are susceptible to hydrogen damage, including phase transformations, hydrogen embrittlement, and corrosion. Diffusion of hydrogen in metals provides an intriguing and challenging intellectual problem in addition to the practical impact. Taking into consideration the importance of diffusion process, many experimental measurements have been performed [1–6]. Also, there have been many theoretical efforts to gain diffusion coefficients for multiple materials and the corresponding diffusion mechanisms using fundamental electronic or atomistic approaches [7–10]. In fact, although the diffusion experiments can determine the overall diffusion coefficients, they cannot generally determine the microscopic physical processes involved in the diffusion steps which are quite important for basic understanding and practical applications. Therefore, first-principles calculations, which have been widely used in the study of solid-state diffusion, can help to track the microscopic diffusion processes and provide specific quantitative values, such as formation and migration energies, involved in the diffusion process.

Metal titanium (Ti), which combines high strength and low density, is a suitable material for the application in aircraft construction and aerospace engineering, as well as in the chemical industry. In most cases, titanium and its alloys display excellent resistance to damage. However, due to the strong affinity between titanium and hydrogen that results in a severe deterioration in the mechanical properties, considerable restrictions exist in their applicability under hydrogen-containing environments, where the hydrogen can be supplied by a number of sources, including water vapor, picking acids, and hydrocarbons. Despite the extensive work on diffusion, there is a serious lack of reliable experimental diffusion data on titanium and many other important systems. It is well known that metals of the IV group exhibit phase transition from α -phase (hcp structure) to β -phase (bcc structure) at the reaction temperature, which is 1155 K for Ti. This relatively low transition temperature for Ti makes diffusion experiments difficult to be solely carried within the α -phase. To date, the experimental diffusion coefficients of hydrogen in α -Ti are scattered over many orders of magnitude [1–3], while to our knowledge, systematic *ab initio* studies of hydrogen diffusion in Ti is still lacking in the literature.

The purpose of the present work is to comprehensively investigate the atomic diffusion mechanism of hydrogen and its isotopes (deuterium and tritium) in α -Ti, and to obtain the specific values of the corresponding energy barriers, vibrational free energies, and diffusion coefficients from first principles. In the most general form, the diffusion coefficient is

expressed as

$$D = D_0 e^{-Q/kT}, \quad (1)$$

where Q is the activation energy, D_0 is a pre-factor, and k is the Boltzmann constant. According to the transition state theory (TST) [11, 12], the jump rate is written as

$$\omega = \frac{kT}{h} \frac{Z_{TS}}{Z_0} e^{-\Delta H_m/kT}, \quad (2)$$

where Z_{TS} and Z_0 are partition functions for the transition state and the ground state, respectively, h is the Planck's constant, and ΔH_m is the enthalpy difference of migration between the transition state and the ground state including the thermal electronic contribution. Within the framework of the harmonic approximation, the quantum mechanical partition functions in Eq. (2) can be expressed as

$$\omega = \frac{kT}{h} \frac{\prod_{i=1}^{3N-6} \left[2 \sinh \left(\frac{h\nu_i^0}{2k_B T} \right) \right]}{\prod_{i=1}^{3N-7} \left[2 \sinh \left(\frac{h\nu_i^{TS}}{2k_B T} \right) \right]} e^{-\Delta H_m/k_B T}, \quad (3)$$

where ν_i^{TS} and ν_i^0 are the vibrational frequencies at the transition state and the ground state, respectively. Using the expression of the phonon free energy

$$F_{vib} = -kT \ln Z_{vib} = kT \int_0^\infty g(\nu) \ln \left[2 \sinh \left(\frac{h\nu}{2kT} \right) \right] d\nu, \quad (4)$$

the jump rate can be simply expressed as

$$\omega = \frac{kT}{h} e^{-\Delta F_{vib}/kT} e^{-\Delta H_m/kT}, \quad (5)$$

where the zero-point energy is included in the F_{vib} term.

As depicted in Fig. 1, there are two stable interstitial positions, i.e., the tetrahedral (T) site and octahedral (O) site, respectively. In the present work we focus on the dual occupancy case. Thus, four jump frequencies are to be considered. In the hcp-structured α -Ti, there are two kinds of impurity jumps, viz. one perpendicular to c axis and the other along the c axis, resulting in two diffusion coefficients which can be expressed as [13]

$$D_\perp = \frac{\omega_{TO}\omega_{OT}}{\omega_{TO} + 2\omega_{OT}} a^2, \quad (6)$$

and

$$D_\parallel = \frac{\omega_{TO}(3\omega_{OO}\omega_{TO} + 2\omega_{OO}\omega_{TT} + 3\omega_{TT}\omega_{OT})}{4(2\omega_{TT} + 3\omega_{TO})(\omega_{TO} + 2\omega_{OT})} c^2, \quad (7)$$

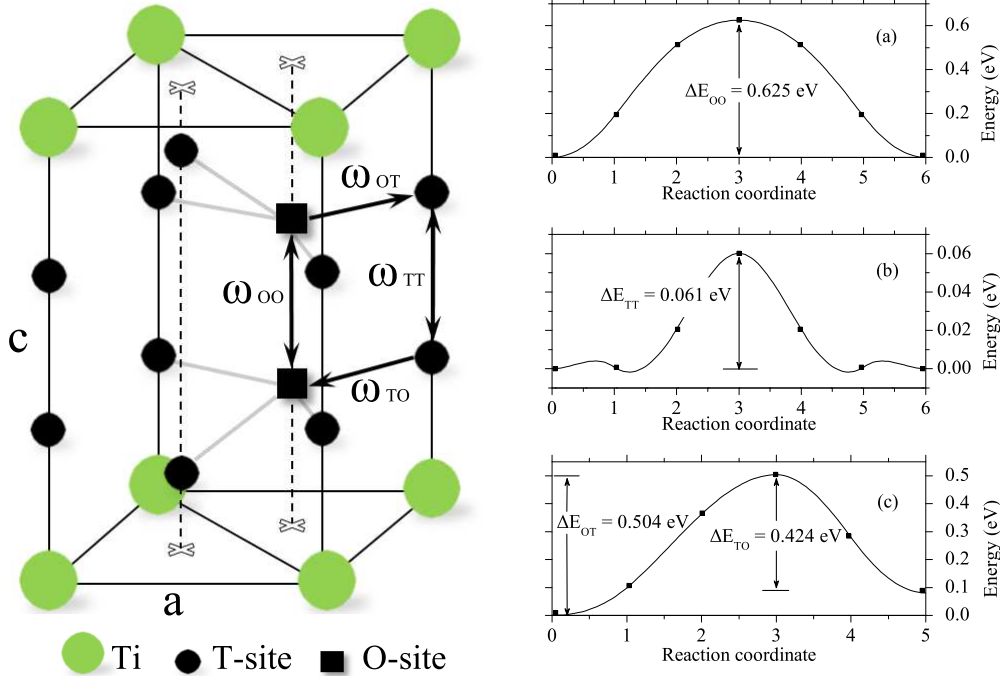


FIG. 1: The arrangement of interstices in the hcp lattice (left panel) and the energy profiles for a hydrogen atom to diffuse along (a) O→O, (b) T→T, and (c) O→T and T→O paths.

where ω_{TO} , ω_{OT} , ω_{OO} , and ω_{TT} are respectively the jump rates along the four paths shown in Fig. 1.

The density functional theory (DFT) calculations are carried out using the Vienna *ab-initio* simulation package (VASP) [14, 15] with the projector-augmented-wave (PAW) potential method [16]. The cutoff energy for the plane-wave basis set is 450 eV. The exchange and correlation effects are described by the generalized gradient approximation (GGA) in the Perdew-Burke-Ernzerhof (PBE) form [17]. We employ a $3 \times 3 \times 2$ α -Ti supercell containing 36 host atoms to simulate hydrogen migration in the α -Ti matrix. To check the convergence of the formation and migration energies, we have also considered a $4 \times 4 \times 3$ α -Ti supercell containing 96 host atoms and one hydrogen atom. The integration over the Brillouin zone is carried out on $3 \times 3 \times 3$ k-point meshes generated using the Monkhorst-Pack [18] method, which proves to be sufficient for energy convergence of less than 1.0×10^{-4} eV per atom. During the supercell calculations, the shape and size of the supercell are fixed while all the ions are free to relax until the forces on them are less than 0.01 eV \AA^{-1} . The phonon spectra are carried out using the density functional perturbation theory.

The theoretical equilibrium lattice parameters a and c/a for α -Ti are 2.939 \AA and 1.583 \AA ,

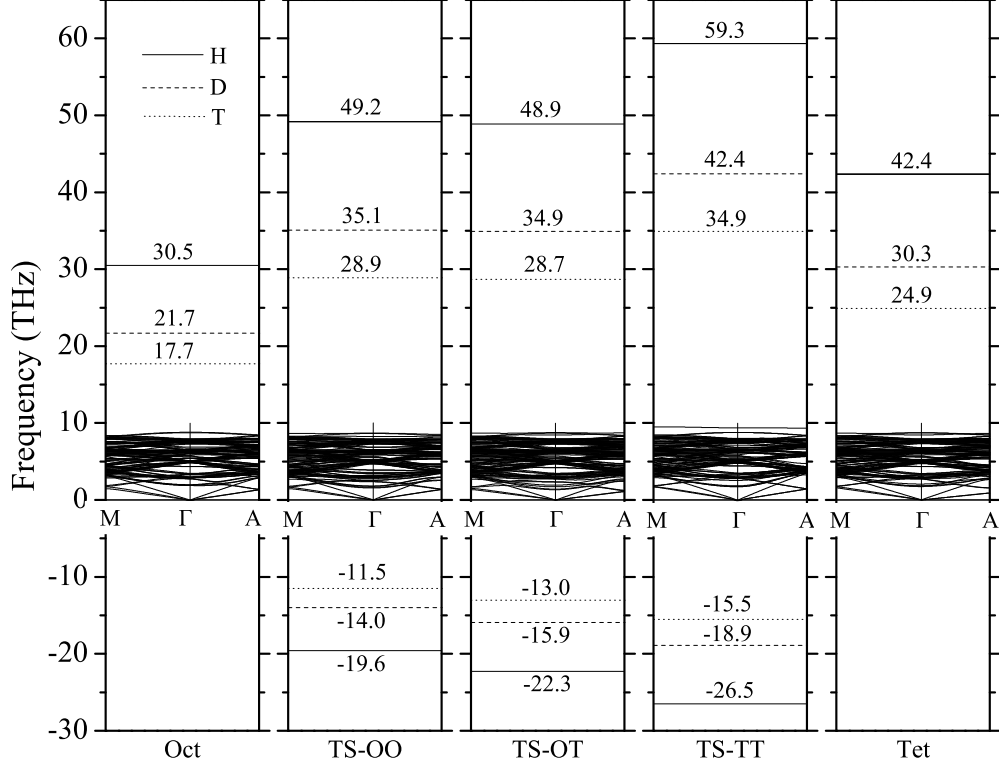


FIG. 2: Calculated phonon dispersions of a 36-atom α -Ti supercell with hydrogen, deuterium, and tritium atoms in the stable octahedral site (Oct), the transition states along the O \rightarrow O (TS-OO), O \rightarrow T (TS-OT), and T \rightarrow T (TT-TS) paths, and the metastable tetrahedral site (Tet), respectively. The modes with imaginary frequencies at the transition states correspond to the motion of the hydrogen, deuterium, and tritium atoms across the barriers.

respectively, in accordance with the experimental data of 2.950-2.957 Å and 1.585-1.587 [19–21]. By comparing the formation energies of a hydrogen defect in O-site and T-site, we find that the O-site is more favorable in energy, lower than the T-site with a 36-atom supercell by 0.080 eV. The 96-atom supercell gives the essentially same result with an energy difference of 0.082 eV. For the calculation of migration energies and phonon frequencies, an important issue concerns the location of the saddle-point position for hydrogen atom. Here, each saddle-point structure and the associated minimum-energy pathway (MEP) were calculated by employing the climbing image nudged elastic band (CINEB) method [22]. As displayed in Fig. 1(a)-(c), when hydrogen atom diffuses from the stable site to the transition site (TS), the energy profile can be well described by a sinusoidal curve, as originally suggested by Wert and Zener [23]. In the case of O \rightarrow O path and T \rightarrow T path, the energy is found to display a

TABLE I: Calculated migration enthalpy difference ΔH_m of atomic hydrogen diffusion via O \rightarrow O path, T \rightarrow T path, O \rightarrow T path, and T \rightarrow O path for $3 \times 3 \times 2$ and $4 \times 4 \times 3$ hcp Ti supercell models, respectively.

	$3 \times 3 \times 2$				$4 \times 4 \times 3$			
	O-O	T-T	O-T	T-O	O-O	T-T	O-T	T-O
ΔH_m	0.662	0.042	0.525	0.439	0.625	0.061	0.504	0.424

single maximum, corresponding to a saddle point at the high-symmetry position located half way between neighboring sites. When hydrogen atom diffuses along the O \rightarrow T path or T \rightarrow O path, the transition state locates close to the T site, and the distance between the saddle point and T-site (O-site) is 0.852 Å (1.001 Å). In Table I, we listed the migration energies of the four diffusion paths using 36- and 96-atom models, respectively. By comparison of the two models, one can see that a 36-atom supercell is already convergent. Actually, the difference in migration energy of these two models are 0.04 eV at most for O \rightarrow O path, indicating that a 36-atom supercell can be reliably used in the simulations of the single hydrogen diffusion energetics. Thus, in the follows we adopt a 36-atom supercell to perform the phonon dispersion calculations.

The phonon dispersions of the 36-atom supercell with a hydrogen atom at the O-site, T-site, and three TS sites are shown in Fig. 2. When a hydrogen atom occupies an octahedral site, its phonons show a threefold-degenerate dispersionless branch at 30.5 THz. At the T-site, the frequencies of the hydrogen atom show a similar character with respect to those in the O-site, and the threefold-degenerate branch moves to 42.4 THz. In both cases, the frequencies are positive, indicating a true minimum in the energy. When the hydrogen atom moves to a transition state, its phonon branches, as shown in Fig. 2, are split into a degenerate doublet, which shift upwards to some extent, and a non-degenerate singlet, which shifts downwards so as to be imaginary, implying the spontaneous diffusion instability for the defective hydrogen in the transition state. By definition, the transition state is characterized by the occurrence of one negative eigenvalue in the dynamical matrix. Here the doublet modes at positive frequency correspond to the vibrations of the hydrogen atom perpendicular to the diffusion path, while the singlet mode at imaginary frequency corresponds to the motion of the hydrogen atom along its diffusion path.

TABLE II: Calculated diffusion pre-factors ($D_{0\perp}$ and $D_{0\parallel}$) and activation energy (Q_{\perp} and Q_{\parallel}) for atomic hydrogen, deuterium, and tritium in α -Ti. The temperatures represent the ranges over which diffusion coefficients were fit to extract corresponding pre-factors and activation energies. For comparison, experimental results are also listed.

Method	$D_{0\perp}$ (m ² /s)	$D_{0\parallel}$ (m ² /s)	Q_{\perp} (kJ/mol)	Q_{\parallel} (kJ/mol)	T (K)
Hydrogen	2.506×10^{-6}	1.275×10^{-6}	51.90	49.89	280-1000
Deuterium	1.587×10^{-6}	8.630×10^{-7}	50.30	48.50	280-1000
Tritium	1.219×10^{-6}	6.781×10^{-7}	49.59	47.85	280-1000
Expt. ^a	1.672×10^{-6}		51.80		773-1097
Expt. ^b	3.057×10^{-6}		62.46		884-1102

^a Reference [1], ^b Reference [2]

When the hydrogen defect locates at the transition state along the T→T path, we note that the hydrogen-related branch has the highest frequency of 59.3 THz compared to 49.2 THz in O→O path and 48.9 THz in O→T path. In fact, the transition site along the T→T path locates at the geometric center of triangle formed by its three nearest Ti atoms, thus the interstitial space is much more confined with respect to the other two transition states. Besides, there is a phonon branch between 9.0 and 10.0 THz in the transition state along the T→T path, which is obviously off from the bulk of Ti-related phonon branches. This branch is related to motions of Ti atoms, which couple with motions of the H impurity. As we expect, the impurity atom related frequencies decrease with increasing mass from hydrogen to its isotopes (cf. Fig. 2).

Integration of the phonon dispersions over the entire Brillouin zone allows to compute the temperature-dependent enthalpy, entropy, and free energy, which can be used to evaluate the diffusion coefficient according to Eq. (1). In Fig. 3 we showed the Arrhenius plot of the computed diffusion coefficients together with experimental values in Refs. [1–3] for comparison. The diffusion coefficient curves for D_{\perp} and D_{\parallel} are almost indistinguishable below 500 K. With increasing temperature, the value of D_{\perp} becomes somewhat higher than D_{\parallel} . Both of these two diffusion coefficients are in agreement with the experimental data by Wasilewski *et al.* [1] and Papazoglou *et al.* [2] (cf. Fig. 3). By linear fitting of the diffusion coefficient curves, we obtained the diffusion pre-factors ($D_{0\perp}$ and $D_{0\parallel}$) and activation energies

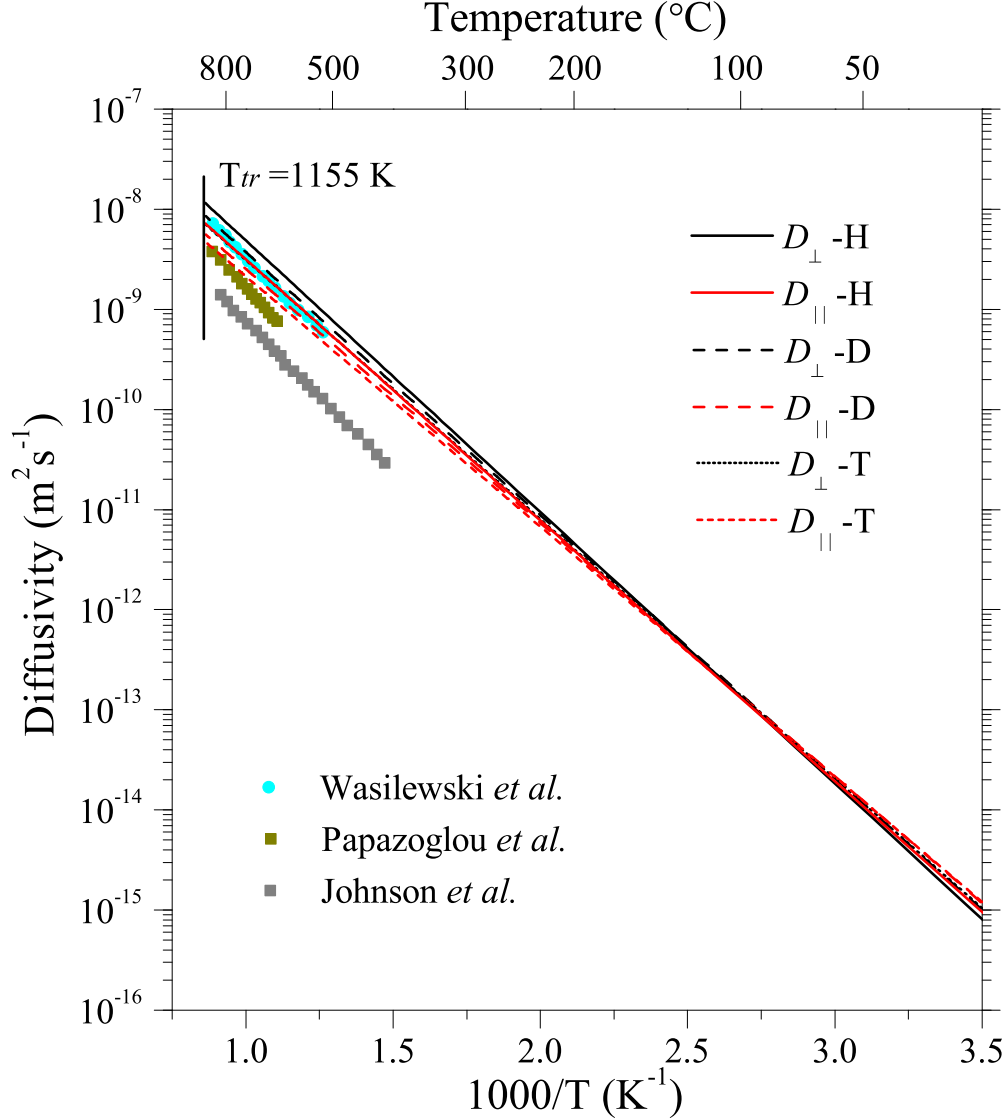


FIG. 3: (Color online) Calculated and experimental diffusion coefficients of atomic hydrogen, deuterium, and tritium in α -Ti. The $T_{tr}=1155$ K stands for the phase transition temperature of metal Ti from α -phase to β -phase.

(Q_{\perp} and Q_{\parallel}) according to the Arrhenius plot of Eq. (1), i.e., $\ln(D) = \ln(D_0) - Q/kT$. In Table 2 we listed our fitting results of pre-factors and activation energies. A linear fit between 280 K and 1000 K of the calculated data for hydrogen gives $Q_{\perp}=51.9$ kJ/mol and $Q_{\parallel}=49.89$ kJ/mol, in agreement with experimental data ranging from 51.80 kJ/mol to 62.46 kJ/mol [1, 2]. The pre-factors are $D_{0\perp}=2.506 \times 10^{-6}$ m²/s and $D_{0\parallel}=1.275 \times 10^{-6}$ m²/s, respectively. One can see that $D_{0\parallel}$ is nearly the half of $D_{0\perp}$. The value of $D_{0\perp}$ is well located in the experimental range from 1.672×10^{-6} m²/s to 3.057×10^{-6} m²/s.

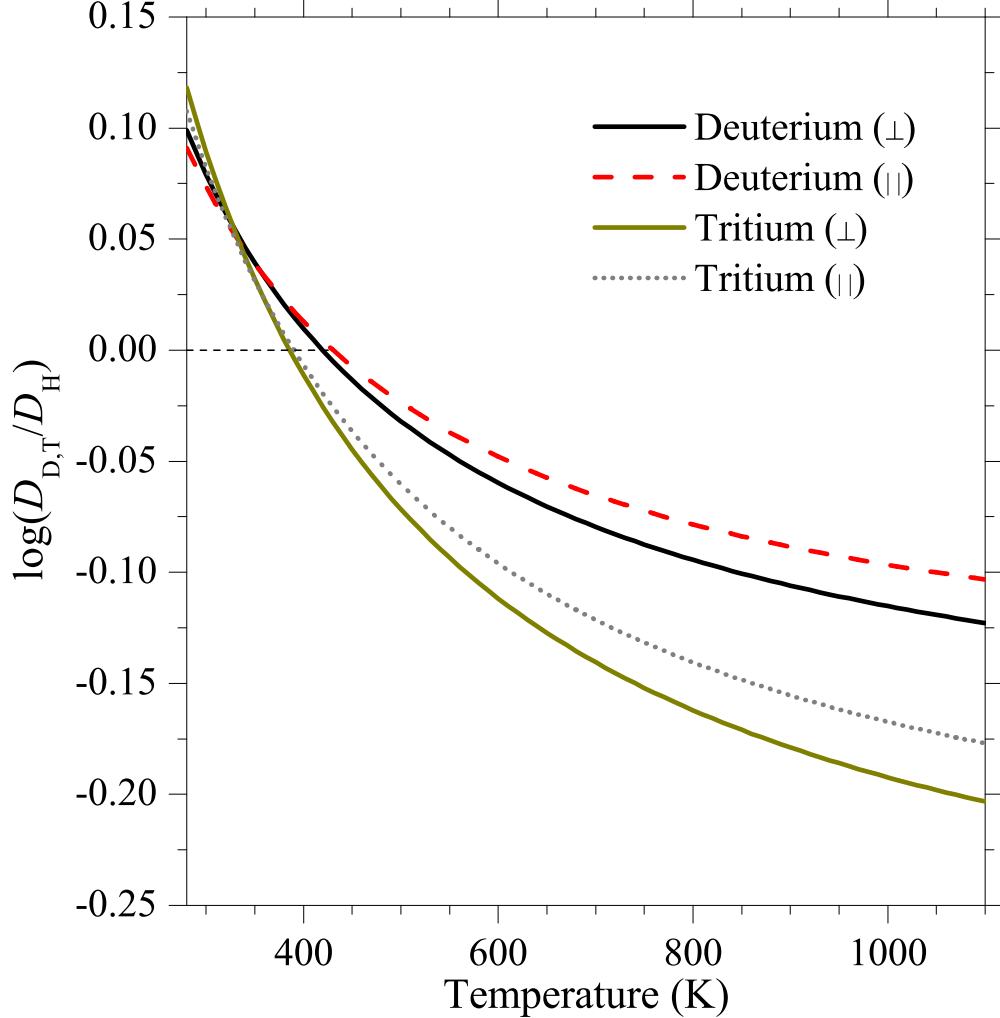


FIG. 4: (Color online) The ratios of the diffusivity of deuterium and tritium to hydrogen atoms. (\perp) and (\parallel) represent the impurity diffusions perpendicular to and parallel to c axis, respectively.

The temperature-dependent diffusion coefficients for the isotopes deuterium and tritium in α -titanium can be calculated based on the electronic structure results of hydrogen in titanium. One would expect a lower diffusivity for the heavier isotopes, since the impurity-related frequencies decrease with increasing mass (Fig. 2). In Fig. 4 we depicted the ratio of the diffusivity of deuterium and tritium to hydrogen. One can see clearly that this is only the case at temperatures above 425 K for deuterium and 390 K for tritium. At lower temperatures, the ordering is reversed. The reason is that at low temperatures, the zero-point energy effect is more pronounced [7], which increases the jump rate through an exponential dependence, since the energy difference between the transition and ground states shows a reduction trend from hydrogen to its isotopes. As the temperature increases,

the zero-point energy effect is offset due to the lower frequencies of isotopes. At 425 K, these two effects achieve a balance for deuterium. Also, a crossover temperature of 390 K is predicted for tritium, as depicted in Fig. 4.

In summary, we have systematically studied the temperature-dependent diffusion coefficients of atomic hydrogen and its isotopes in α -Ti using transition state theory with accurate first-principle total energy and phonon calculations. The quantitative agreement between the calculated and experimental diffusion coefficients has been achieved, which demonstrates the validity and practicability of the present theoretical method. Our calculated ratios of the diffusivity of isotopes and hydrogen provide a good reference for future experimental measurements on α -Ti.

This work was supported by NSFC under Grant No. 51071032 and by CAEP Foundations for Development of Science and Technology under Grant No. 2011A0301016.

-
- [1] R. J. Wasilewski and G. L. Kehl, *Metallurgica*, **50** (1954) 225-230.
 - [2] T. P. Papazoglou and M. T. Hepworth, *Trans. Met. Soc. AIME*, **242** (1968) 682-685.
 - [3] D. L. Johnson and H. G. Nelson, *Met. Trans.*, **4** (1974) 533-542.
 - [4] J. Völkl and G. Alefeld, in *Hydrogen in Metals*, edited by G. Alefeld and J. Völkl (Springer, New York, 1978).
 - [5] Y. Ebisuzaki, W. J. Kass, and M. O’Keeffe, *J. Chem. Phys.* **46** (1967) 1373.
 - [6] L. Katz, M. Guinan, and R. J. Borg, *Phys. Rev. B* **4** (1971) 330.
 - [7] E. Wimmer, W. Wolf, J. Sticht, and P. Saxe, *Phys. Rev. B* **77** (2008) 134305.
 - [8] M. Mantina, Y. Wang, R. Arroyave, L. Q. Chen, Z. K. Liu, and C. Wolverton, *Phys. Rev. Lett.* **100** (2008) 215901.
 - [9] M. Mantina, Y. Wang, L. Q. Chen, Z. K. Liu, and C. Wolverton, *Acta Mater.* **57** (2009) 4102-4108.
 - [10] G. Y. Huang, C. Y. Wang and J. T. Wang, *Scripta Mater.* **61** (2009) 324-326.
 - [11] H. Eyring, *J. Chem. Phys.* **3** (1935) 107.
 - [12] G. H. Vineyard, *J. Phys. Chem. Solids* **3** (1957) 121.
 - [13] S. Ishioka and M. Koiwa, *Philos. Mag. A* **52** (1985) 267-277.
 - [14] G. Kresse and D. Joubert, *Phys. Rev. B* **59**(1999) 1758.

- [15] G. Kresse and J. Furthmüller, Phys. Rev. B **54** (1996) 11169.
- [16] P. E. Blöchl, Phys. Rev. B **50** (1994) 17953.
- [17] J. P. Perdew, K. Burke and M. Ernzerhof, Phys. Rev. Lett. **77** (1996) 3865.
- [18] H. J. Monkhorst and J. D. Pack, Phys. Rev. B **13** (1976) 5188.
- [19] Y. K. Vohra, P. T. Spencer, Phys. Rev. Lett. **86** (2001) 3068.
- [20] S. A. Ostanin and V. Y. Trubitsin, J. Phys.: Condens. Matter **9**, (1997) L491.
- [21] J. Z. Zhang, Y. Zhao, R. S. Hixson, G. T. Gray, L. P. Wang, W. Utsumi, S. Hiroyuki, and H. Takanori, Phys. Rev. B **78** (2008) 054119.
- [22] G. Henkelman, B. P. Uberuaga and H. Jonsson, J. Chem. Phys. **113** (2000) 9901.
- [23] C. Wert and C. Zener, Phys. Rev. **76** (1949) 1169.